Transcript Level Modulates the Inherent Oncogenicity of RET/PTC Oncoproteins

Douglas S. Richardson,[1] Taranjit S. Gujral,[1] Susan Peng,[1] Sylvia L. Asa,[2] and Lois M. Mulligan[1]

[1]Department of Pathology and Molecular Medicine, Division of Cancer Biology and Genetics, Cancer Research Institute, Queen's University, Kingston, Ontario, Canada and [2]Department of Pathology, University Health Network, Ontario Cancer Institute, Toronto, Ontario, Canada

Abstract

Mutations to the *RET* proto-oncogene occur in as many as one in three cases of thyroid cancer and have been detected in both the medullary (MTC) and the papillary (PTC) forms of the disease. Of the nearly 400 chromosomal rearrangements resulting in oncogenic fusion proteins that have been identified to date, the rearrangements that give rise to RET fusion oncogenes in PTC remain the paradigm for chimeric oncoprotein involvement in solid tumors. RET-associated PTC tumors are phenotypically indolent and relatively less aggressive than RET-related MTCs. The mechanism(s) contributing to the differences in oncogenicity of RET-related MTC and PTC remains unexplained. Here, through cellular and molecular characterization of the two most common RET/PTC rearrangements (PTC1 and PTC3), we show that RET/PTC oncoproteins are highly oncogenic when overexpressed, with the ability to increase cell proliferation and transformation. Further, RET/PTCs activate similar downstream signaling cascades to wild-type RET, although at different levels, and are relatively more stable as they avoid lysosomal degradation. Absolute quantitation of transcript levels of *RET, CCDC6*, and *NCOA4* (the 5′ fusion genes involved in PTC1 and PTC3, respectively) suggest that these rearrangements result in lower RET expression in PTCs relative to MTCs. Together, our findings suggest PTC1 and PTC3 are highly oncogenic proteins when overexpressed, but result in indolent disease compared with RET-related MTCs due to their relatively low expression from the *NCOA4* and *CCDC6* promoters *in vivo*. [Cancer Res 2009;69(11):4861–9]

Introduction

The *RET* proto-oncogene encodes a receptor tyrosine kinase (RTK) that is widely expressed in neuroendocrine tissues and is essential for embryonic development of the kidney and enteric nervous system (reviewed in ref. 1). Sporadic and germ-line mutations of *RET* have been associated with the initiation of thyroid carcinoma. Point mutations of key residues have been linked to medullary thyroid carcinoma (MTC) and the inheritable cancer syndrome multiple endocrine neoplasia type 2 (MEN 2), whereas chromosomal rearrangements involving *RET* result in papillary thyroid carcinoma (PTC; refs. 2–4; reviewed in refs. 5, 6). Although the common underlying initiator of tumor growth appears to be constitutive activation of the RET kinase, the molecular mechanisms that result in RET activation and the pathophysiology of these tumors vary widely.

RET-related MTCs arise from the C-cells of the thyroid and are characterized by early onset and metastasis to lymph nodes and distant organs (7). These tumors are primarily associated with single amino acid substitutions in the intracellular kinase domain or extracellular cysteine residues of RET that result in a constitutively active molecule (2, 3). RET-related PTCs are highly heterogeneous tumors of thyroid follicular cells. They generally present as indolent tumors that rarely exhibit lymph node invasion or metastasis to distant organs (7, 8). Endogenous *RET* is expressed at very low levels in thyroid follicular cells relative to C-cells (9); however, in ~30% to 40% of PTCs (10–12), chromosomal rearrangements involving the *RET* gene fuse the 5′ sequences and promoter of an ubiquitously expressed gene upstream of the *RET* kinase domain, leading to expression of a chimeric product, a RET/PTC (reviewed in refs. 5, 6). RET/PTCs are localized to the cytoplasm, as they lack the NH_2-terminal signal sequence and transmembrane domain of RET. All NH_2-terminal fusion partners identified to date contain homodimerization domains that mediate dimerization and activation of the kinase region in RET/PTC oncoproteins. The most common RET/PTC rearrangements, PTC1 and PTC3, link *RET* to the genes *CCDC6* and *NCOA4*, respectively.

To determine the mechanistic explanation for the relatively indolent phenotype of RET/PTC tumors compared with RET-related MTCs, we examined the oncogenic potential of RET/PTCs both *in vitro* and *in vivo* at the cellular and molecular levels. We show that, when overexpressed, RET/PTCs display properties similar to constitutively active, membrane-bound RET mutants such as high levels of phosphorylation, presence in high molecular weight native protein complexes, activation of similar cell growth and proliferation signaling cascades, and ability to increase cell proliferation and cause transformation. Further, the cytoplasmic enrichment of RET/PTCs uncouples them from receptor-mediated endocytosis and lysosomal degradation, leading to increased protein stability. In contrast, *in vivo* investigation of transcript levels in seven human cell lines suggested that expression of RET/PTCs via the 5′ promoter regions of *CCDC6* or *NCOA4* could result in lower expression of these oncoproteins, relative to full-length RET, expressed off its endogenous promoter in thyroid C-cells.

Together, our results suggest that RET/PTCs possess similar or greater oncogenic potential than membrane-bound RET when expressed at similar levels; however, *in vivo*, this is trumped by substitution of relatively weak promoters upstream of the chimeric oncogene. These data suggest that careful consideration of multiple cellular mechanisms is required to determine the oncogenic potential of the many fusion proteins implicated in human cancer.

Requests for reprints: Lois M. Mulligan, Department of Pathology and Molecular Medicine, Division of Cancer Biology and Genetics, Cancer Research Institute, Queen's University, Room A315, Botterell Hall, Kingston, Ontario, Canada K7L 3N6. Phone: 613-533-6000, ext. 77475; Fax: 613-533-6830; E-mail: mulligal@queensu.ca.

doi:10.1158/0008-5472.CAN-08-4425

Materials and Methods

Cell culture and transfections. HEK 293 Tet-on, HeLa, TPC1, MIA-PaCa 2, SK-N-SH, and TT cells were grown in DMEM (Sigma-Aldrich). ARO cells were cultured in RPMI 1640 supplemented with 2 mmol/L L-glutamine, 1 mmol/L sodium pyruvate, and 1× nonessential amino acids. KTC1 and 8505C cells were maintained in RPMI 1640 with 2 mmol/L L-glutamine. All cell cultures were supplemented with 10% fetal bovine serum and 1 μmol/L AP20187 artificial dimerizer (Ariad Pharmaceuticals) and doxycycline (1 μg/mL) was added after transfection. All transfections were done transiently using Lipofectamine 2000 (Invitrogen).

Immunoprecipitation, immunoblotting, and densitometry. Immunoprecipitation and immunoblotting were done according to previously published methods (13). Briefly, lysed cells were separated into cytosolic and membrane-associated fractions by centrifugation at 12,000 × *g*. Cytosolic fractions were immunoprecipitated with 0.8 μg antibody and 20 μL protein A/G slurry (Santa Cruz Biotechnology). Lysates and immunoprecipitates were separated by 10% SDS-PAGE, transferred to nitrocellulose, and immunoblotted. Mean pixel intensity of areas surrounding the 175 and 155 kDa bands of wild-type RET, the single bands of RET-IC, PTC1 and PTC3, both extracellular signal-regulated kinase (ERK) 1 and 2 bands, or the entire ubiquitin smear was determined by densitometry using ImageJ software (19).

Antibodies and constructs. Antibodies used included anti-RET, LAMP2, HA-tag, ERK, and phospho-ERK from Santa Cruz Biotechnology. Phospho-RET Y905 and phospho-STAT3 Y705 were from Cell Signaling Technology. Phospho-β-catenin Y654 antibody was developed by Drs. Janne Balsamo and Jack Lilien and was obtained from the Development Studies Hybridoma Bank, developed by the National Institute of Child Health and Human Development, and maintained at the University of Iowa. Full-length wild-type RET, RET K758M, and GFRα1 constructs have been described previously (14). Empty vector (EV) refers to pcDNA3.1 plasmid (Invitrogen). RET-IC was cloned by fusing the intracellular domain of RET (amino acids 658-1,072) via a linker sequence (GGGGS × 3) to a FKBP domain and NH_2-terminal myristoylation signal. PTC1, PTC3, and HA-tagged c-CBL, CBL-b, and ubiquitin constructs have been described previously (15–18).

Confocal microscopy. HeLa cells were fixed and stained as described previously (14). Individual images were obtained with a Leica TCS-SP2 inverted microscope. After acquisition, images were background subtracted (removal of pixel intensities <30) and merged using ImageJ software (19). Colocalization was determined using the "ImageJ RG2B colocalization" (Christopher Philip Mauer) and "Mander's coefficient" (from the MBF collection by Tony Collins) plug-ins.[3]

Size exclusion chromatography. This method was done as described previously (20). 293 Tet-on cell lysate (~1.5 mg) expressing RET-IC, PTC1, or PTC3 was loaded at room temperature onto a Superdex 200 column (GE Healthcare) equilibrated with TBS solution (pH 7.2; 25 mmol/L Tris, 50 mmol/L NaCl). Fractions (2 mL) were collected and separated by SDS-PAGE and immunoblotted for RET and ERK1/2. Approximate molecular weights of native proteins contained in each fraction were estimated as described previously (20).

Cell proliferation assay. Transfected cells were seeded in 96-well plates at a density of 5×10^3 per well. Four days post-seeding, 200 ng/mL 3-(4,5-dimethylthiazol-2-yl)-2,5-diphenyltetrazolium bromide (MTT; Sigma) was added for 3 h. Cells were resuspended in 24:1 isopropanol to 1 N HCl (v/v), and absorbance was measured at 570 nm.

Colony formation assay. Colony formation assays were done as described previously (13). Approximately 2×10^4 cells were resuspended in 0.2% top agar in DMEM and plated on 0.4% bottom agar in medium. Fetal bovine serum, doxycycline, and dimerizer were added in both layers. Colonies were counted after 15 days.

Cyclohexamide protein stability assays. Previously transfected 293 HEK Tet-on cells were seeded in 6-well plates. Cyclohexamide (100 μg/mL; Bioshop) was added to each sample for indicated times. Wild-type RET and RET K758M were cotransfected with GFRα1, and 50 ng/mL glial cell-derived neurotrophic factor (Peprotech) was added along with cyclohexamide. Equal amounts of protein, as determined by BCA Assay (Fisher), from each sample were separated by SDS-PAGE and immunoblotted for RET.

Ubiquitination assay. MG132 (10 μmol/L; Sigma) was added to cells for 30 min. Cell lysates were immunoprecipitated with anti-RET antibody. The intensity of smears in EV control lanes (background) was subtracted and mean pixel intensities were normalized to total RET protein in the immunoprecipitates.

PCR. PCR was done using GO-Taq all-in-one PCR mix (Fisher) according to the manufacturer's instructions.

Quantitative real-time PCR. RNA was harvested using TRizol reagent (Invitrogen). RNA was reverse transcribed and amplified using the one-step QuantiTect SYBR Green Real-time PCR kit (Qiagen). Crossing threshold (Ct) values were determined by SmartCycler II software. mRNA copy numbers were estimated by solving equations defining standard curves (created using *RET, CCDC6*, and *NCOA4* linearized plasmid DNA) using Ct values obtained from each of our cell lines using the *RET* 3′, *NCOA4* 5′, and *CCDC6* 5′ primer pairs (Supplementary Table S1).

Statistical analysis. Data are expressed as mean ± SD. A two-tailed, unpaired Student's *t* test was used to determine statistical significance.

Results and Discussion

RET-IC phosphorylates, dimerizes, and targets to the plasma membrane. To determine the *in vitro* oncogenic potential of RET/PTCs, expression constructs encoding PTC1 and PTC3 were transiently overexpressed in mammalian cells and compared on both cellular and molecular levels with a constitutively active MEN 2-like membrane-bound construct, RET-IC (Fig. 1*A*). RET-IC encodes the intracellular domain of RET fused downstream of a FKBP dimerization domain and the plasma membrane targeting myristoylation signal of Src (ref. 21; Fig. 1*A*). Cellular fractionation experiments show that total and phospho-PTC1 and PTC3 were enriched in cytosolic fractions, whereas a relatively greater amount of RET-IC was found to be membrane-associated (Fig. 1*B*; full-length wild-type RET also distributed to both fractions; data not shown). In whole cells, PTC1 and PTC3 were diffusely distributed throughout the cytoplasm in comparison to RET-IC, which was concentrated at the plasma membrane and in punctate intracellular structures (Fig. 1*C*). Size exclusion chromatography of native proteins from cleared cell lysates was used to determine whether RET-IC, PTC1, and PTC3 showed similar levels of dimerization. We found RET-IC, PTC1, and PTC3 were all present as high molecular weight complexes within the cell (Fig. 1*D*). Monomeric forms of these proteins were nearly undetectable, unlike ERK1/2, which was found in both low and high molecular weight fractions (Fig. 1*D*), as reported by others (22). This experiment, along with the phosphorylation data in Fig. 1*B*, suggests that RET-IC, PTC1, and PTC3 dimerize rapidly after translation and exist in complex with multiple adaptor and effector proteins.

PTC1 and PTC3 possess oncogenic potential. The effect of PTC1 and PTC3 expression on cellular proliferation and transformation was assessed in comparison with RET-IC. Equal and reproducible expression of all three constructs over three independent transient transfections was confirmed by quantitative RT-PCR (qRT-PCR) determination of relative transcript levels. Figure 2*A* shows that transfection of all three plasmids produced similar decreases in the Ct value (increases in expression) relative to cells transfected with an EV, indicating that equal levels of RET-IC, PTC1, and PTC3 transcript were consistently obtained over multiple transfections. MTT assays showed that all three constructs increased cellular proliferation compared with an EV control

[3] http://rsbweb.nih.gov/ij/ and http://www.macbiophotonics.ca/downloads.htm.

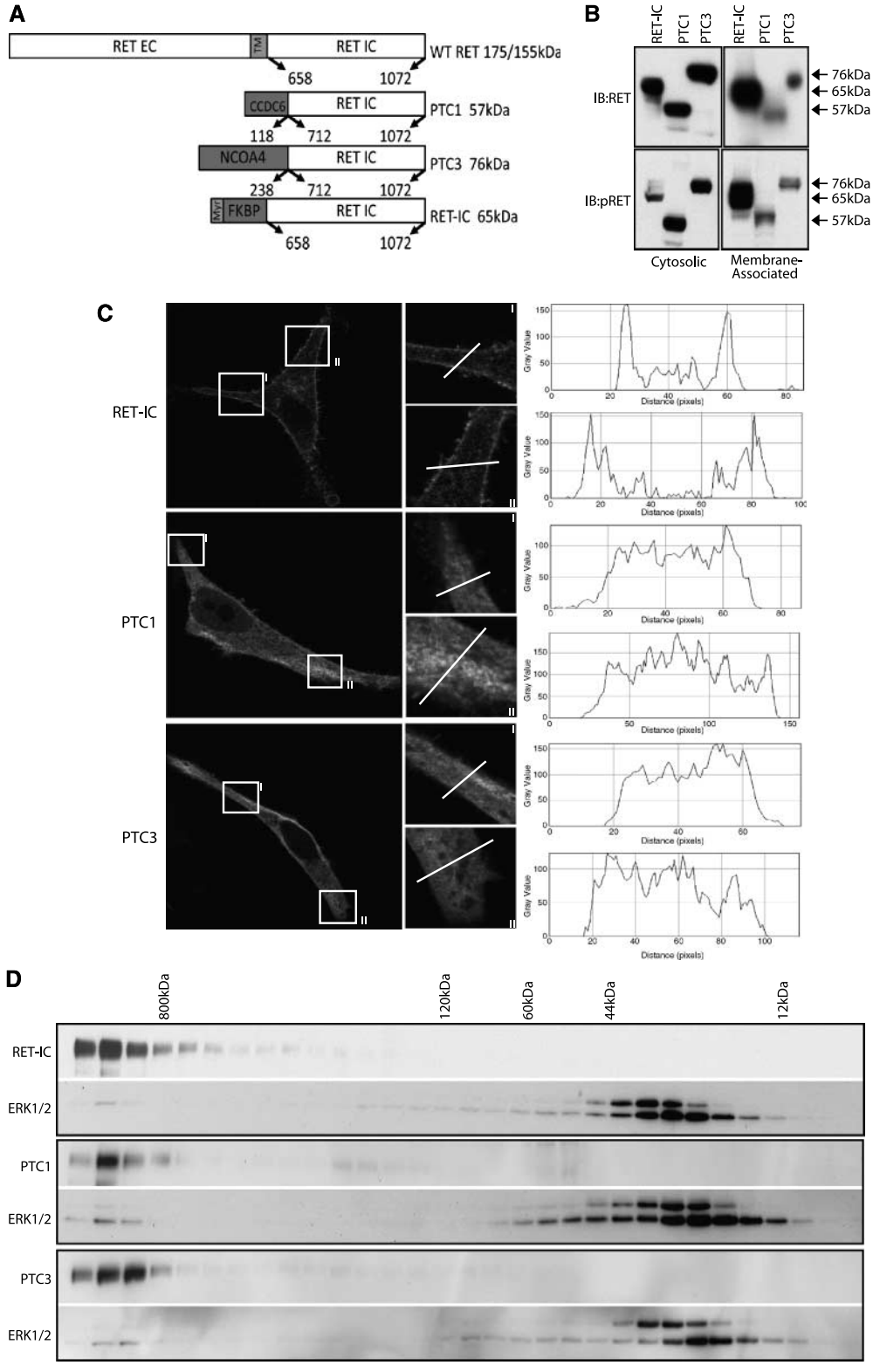

Figure 1. RET-IC phosphorylates, dimerizes, and targets to the plasma membrane. *A,* diagram of constructs used in this study. *IC,* intracellular domain; *TM,* transmembrane domain; *Myr,* myristoylation signal. *B,* transiently transfected HEK 293 Tet-on were separated into cytoplasmic and membrane-associated fractions, separated by SDS-PAGE, and immunoblotted for RET and phospho-RET (*pRET*). *C,* confocal microscopy images of transiently transfected HeLa cells immunostained for RET. *Left,* enlargements correspond to the squares. Pixel intensity histograms along the planes indicated in the enlargements are also presented. *D,* native proteins from transiently transfected cells were separated by size exclusion chromatography. Each fraction was separated by SDS-PAGE and immunoblotted for RET and ERK1/2. Approximate molecular weights corresponding to various fractions are indicated.

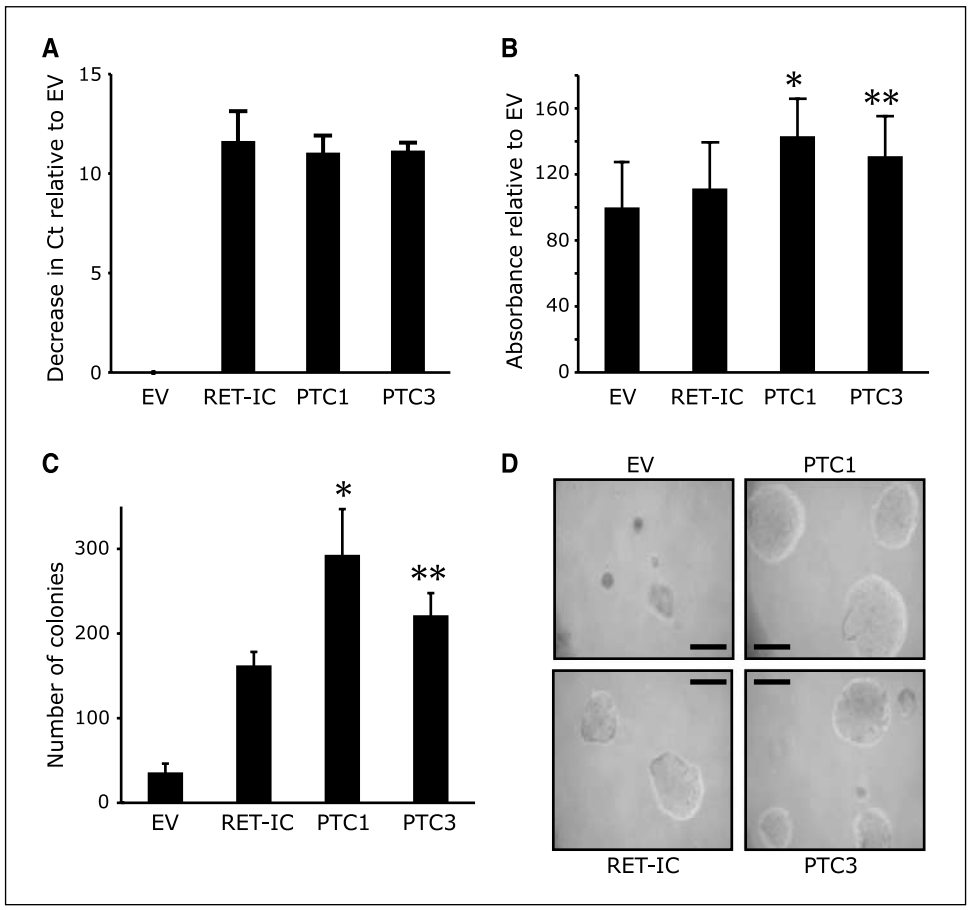

Figure 2. PTC1 and PTC3 are oncogenic when overexpressed. *A,* relative transcript levels of *RET-IC, PTC1*, and *PTC3* were determined by qRT-PCR after transient transfection using common primers to the 3′ tail of all constructs. *EV*, empty vector. Ct values for each sample were calculated and normalized to expression of the housekeeping gene, *GUSB*. Mean ± SD decrease in Ct value relative to EV (mean Ct EV - mean Ct RET-IC/PTC1/PTC3) was plotted for each sample. $n = 6$; (transfections were carried out in triplicate; each qRT-PCR was done in duplicate). *B,* MTT assays were done. Mean ± SD increase in absorbance at 570 nm normalized to EV ($n = 16$). *, $P < 0.005$ to RET-IC; **, $P < 0.05$ to RET-IC (unpaired, two-tailed Student's *t* test). *C,* colony formation assays were done in soft agar. Mean ± SD number of colonies ($n = 4$ for EV and PTC1 and $n = 5$ for RET-IC and PTC3). *, $P < 0.002$ to RET-IC; **, $P < 0.003$ to RET-IC (unpaired, two-tailed Student's *t* test). *D,* phase-contrast images of representative colonies from *C*. *Bar*, 400 μm.

(Fig. 2*B*). PTC1 and PTC3 induced a relative increase in cell proliferation over RET-IC; however, the increase was more significant in cells containing the PTC1 oncoprotein than PTC3 ($P < 0.005$ and $P < 0.05$, respectively; Fig. 2*B*). In soft agar assays, RET-IC, PTC1, and PTC3 induced transformation and colony formation (Fig. 2*C* and *D*). Again, PTC1 and PTC3 induced significantly more colonies than RET-IC ($P < 0.002$ and $P < 0.003$, respectively), with PTC1 colonies consistently larger than those induced by PTC3 or RET-IC (Fig. 2*C* and *D*).

RET/PTC mutants avoid lysosomal degradation. Receptor-mediated endocytosis has been shown to play an important role in the down-regulation of RTKs. Through this process, activated receptors are internalized from the plasma membrane and delivered to the lysosome for degradation (reviewed in ref. 23). Previously, we have shown that activated, wild-type RET is internalized by this process (24); however, as canonical receptor-mediated endocytosis requires direct interaction with, or internalization to, a structure of the endocytic pathway for lysosomal delivery (23), we investigated whether the loss of membrane association affected RET/PTC stability within the cell. Direct visualization of cells showed that both PTC1 and PTC3, but not RET-IC, avoid lysosomal targeting. Colocalization of RET-IC, PTC1, or PTC3 with LAMP2, a commonly used marker of lysosomes (25), was quantified using two algorithms. Both composite images of the mean pixel intensity in the RET and LAMP2 channels (Fig. 3*A, Average Colocalization*), and XY scatter plots based on pixel intensity in the RET (*X axis*) and LAMP2 (*Y axis*) channels (Fig. 3*A*) indicated low levels of PTC1 and PTC3 colocalization with LAMP2, whereas RET-IC and LAMP2 were highly colocalized.

To determine the stability of PTC1 and PTC3 relative to RET-IC, a translation inhibition assay was done. Figure 3*B* shows that loss of both immature 155 kDa and mature 175 kDa bands of wild-type RET occurred over time in cells incubated with glial cell-derived neurotrophic factor and the translation inhibitor cyclohexamide, suggesting that wild-type RET is quickly internalized and degraded after activation. A kinase-dead RET mutant, RET K758M, showed a similar decrease in the immature band of RET but an increase in mature RET (Fig. 3*B*), indicating membrane accumulation of nonphosphorylated RET, which cannot be internalized and degraded (24). As expected, RET-IC showed a similar degradation profile to wild-type RET, with >40% reduction in total RET over the course of the experiment, whereas both total and phospho-PTC1 levels remained relatively stable over the 8 h time course (Fig. 3*C* and *D*). Surprisingly, PTC3 showed a 30% reduction in total protein over the 8 h time course (Fig. 3*C* and *D*), relatively less than the reduction in RET-IC, but unexpected as PTC3 was shown to avoid lysosomal targeting (Fig. 3*A*). This would suggest that an alternate mechanism of PTC3 degradation exists that is less efficient than degradation of membrane-bound RET mediated by the lysosome. The primary site of cytosolic protein degradation, and the most likely candidate for PTC3 down-regulation, is the proteasome. However, the observation that PTC3, although degraded, is still more stable than RET-IC suggests that it does not have a high degree of affinity for this process.

PTC1 and PTC3 differ in downstream signaling and CBL interactions. Activation of downstream signaling cascades known

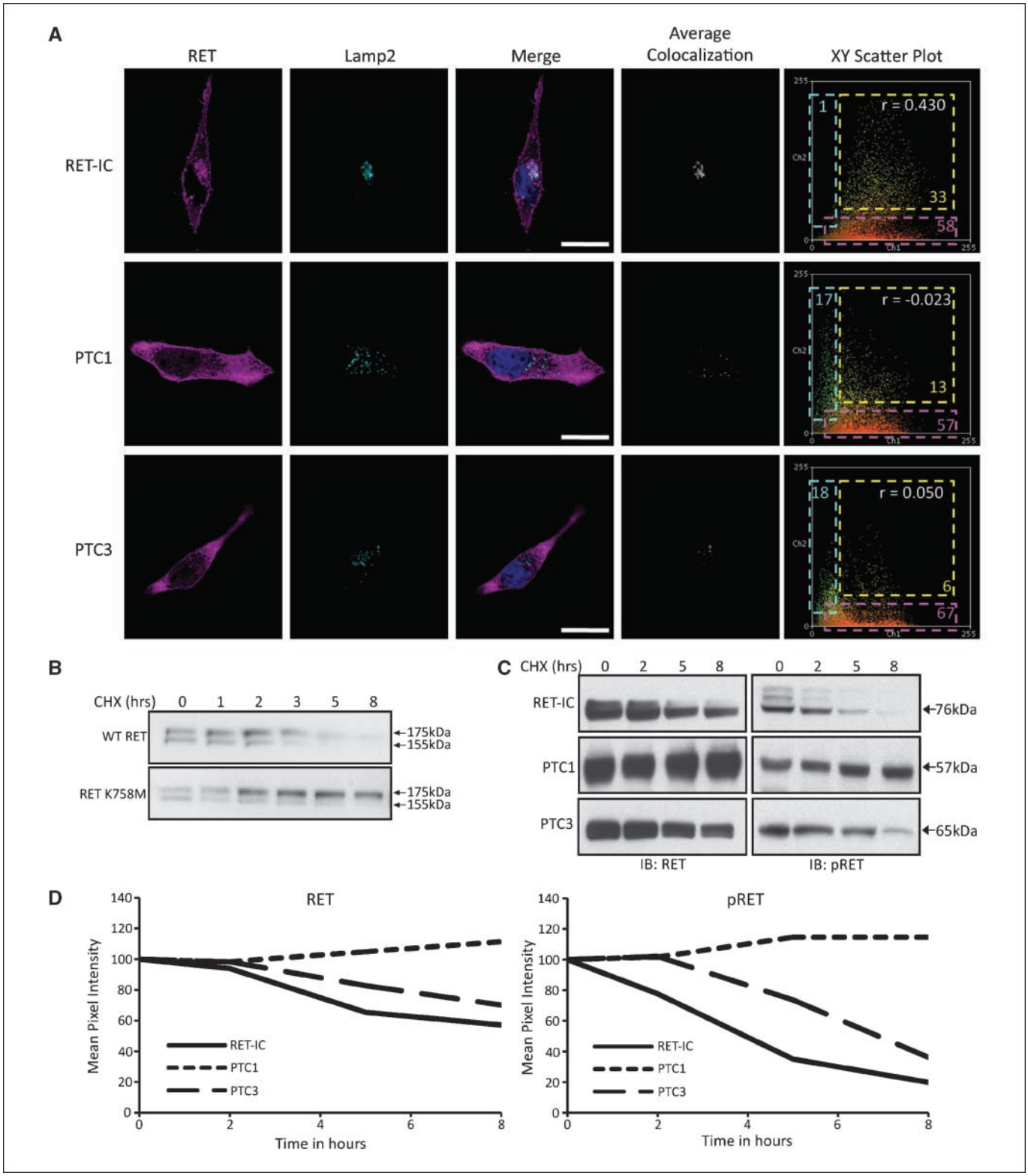

Figure 3. PTC1 and PTC3 avoid lysosomal degradation. *A,* transiently transfected HeLa cells were immunostained for RET (*magenta*) and LAMP2 (*cyan*). Nuclei were counterstained with Hoechst (*blue*). *Average Colocalization,* grayscale image of the mean intensity of colocalized magenta and cyan pixels. *XY Scatter Plots,* pixel intensity (0-255) in the magenta channel (Ch.1; *X axis*) versus the intensity of the same pixel in the cyan channel (Ch. 2; *Y axis*). *r,* Pearson correlation coefficient. *Cyan* and *magenta boxes,* pixels in those channels displaying no colocalization with RET or LAMP2, respectively; *yellow boxes,* pixels that contained signal in both RET and LAMP2 channels. The percentage of pixels in each of these boxes is indicated. *Bar*, 20 μm. *B,* cells were transiently transfected with GFRα1 and wild-type (*WT*) RET or RET K758M, incubated for the indicated times with 50 ng/mL glial cell-derived neurotrophic factor and 100 μg/mL cyclohexamide, lysed, and immunoblotted for RET. *C,* cells were transiently transfected and cultured along with AP20187 dimerizer and doxycycline. Cyclohexamide was added for the indicated times before cells were lysed and immunoblotted for RET and phospho-RET. *D,* mean pixel intensity for each corresponding band in (*C*) was measured, normalized to 0 h, and plotted.

to be associated with increased growth and proliferation and interaction with the E3 ubiquitin ligases CBL-b and c-CBL, which are known to modulate RTK signaling, were assessed downstream of RET-IC, PTC1, and PTC3. RET-IC, PTC1, and PTC3 all increased signaling through the ERK/mitogen-activated protein kinase pathway compared with cells transfected with an EV control (Fig. 4*A*). PTC1 induced relatively higher levels of ERK1/2 phosphorylation, whereas PTC3 and RET-IC induced similar levels of phosphorylation (Fig. 4*A*). Interestingly, these data are consistent with those in Fig. 1*D*, where PTC1 appeared to shift a greater amount of ERK1/2 protein into high molecular weight complexes. This shift to higher molecular weight complexes has been previously associated with ERK activation (22). Further, the increased stability of PTC1 within the cytoplasm (Fig. 3*C* and *D*), an area of concentrated ERK signaling, relative to RET-IC and PTC3, may contribute to its increased signaling through this pathway. Increased tyrosine phosphorylation at residue Y654 of β-catenin, a recently identified target of both wild-type RET and RET/PTCs (14, 26, 27), was observed with all three constructs, although the membrane-associated RET-IC induced relatively higher levels than PTC1 and PTC3 (Fig. 4*A*). The increased ability of RET-IC to phosphorylate β-catenin is consistent with its closer association with membrane-localized pools of this molecule. STAT3, a transcription factor involved in cell cycle progression, is tyrosine phosphorylated downstream of RET activation (28). Interestingly, although all three constructs increased STAT3 signaling, PTC3 induced the strongest phosphorylation of STAT3, whereas PTC1 and RET-IC showed similar levels. The NH_2-terminal region of PTC3 that is donated from NCOA4 also contains a putative STAT3 binding site (YXXV/Q) downstream from Y71 (YEQV), which may recruit STAT3 molecules in addition to the previously identified binding sites at Y752 and Y928 in RET. RET-IC, PTC1, and PTC3 did not increase AKT or nuclear factor-κB phosphorylation relative to EV (data not shown); however, HEK 293 Tet-on cells possess intrinsically high levels of prosurvival signaling through AKT and NFκ-B, likely masking the effects of our oncoproteins on these signaling cascades.

Ubiquitination, specifically by CBL, has been well characterized as an "off" switch for downstream signaling, mediating lysosomal targeting of RTKs for degradation (29). c-CBL interacts indirectly with COOH-terminal docking sites on RET that are also present in the RET/PTC oncoproteins, leading to ubiquitination and targeting of RET for degradation (29). We confirmed that c-CBL could coimmunoprecipitate RET-IC but found it unable to coimmunoprecipitate substantial amounts of PTC1 or PTC3 (Fig. 4*B*). Interestingly, CBL-b, a homologue of c-CBL, was able to precipitate RET-IC, although at lower levels relative to c-CBL, as well as substantial

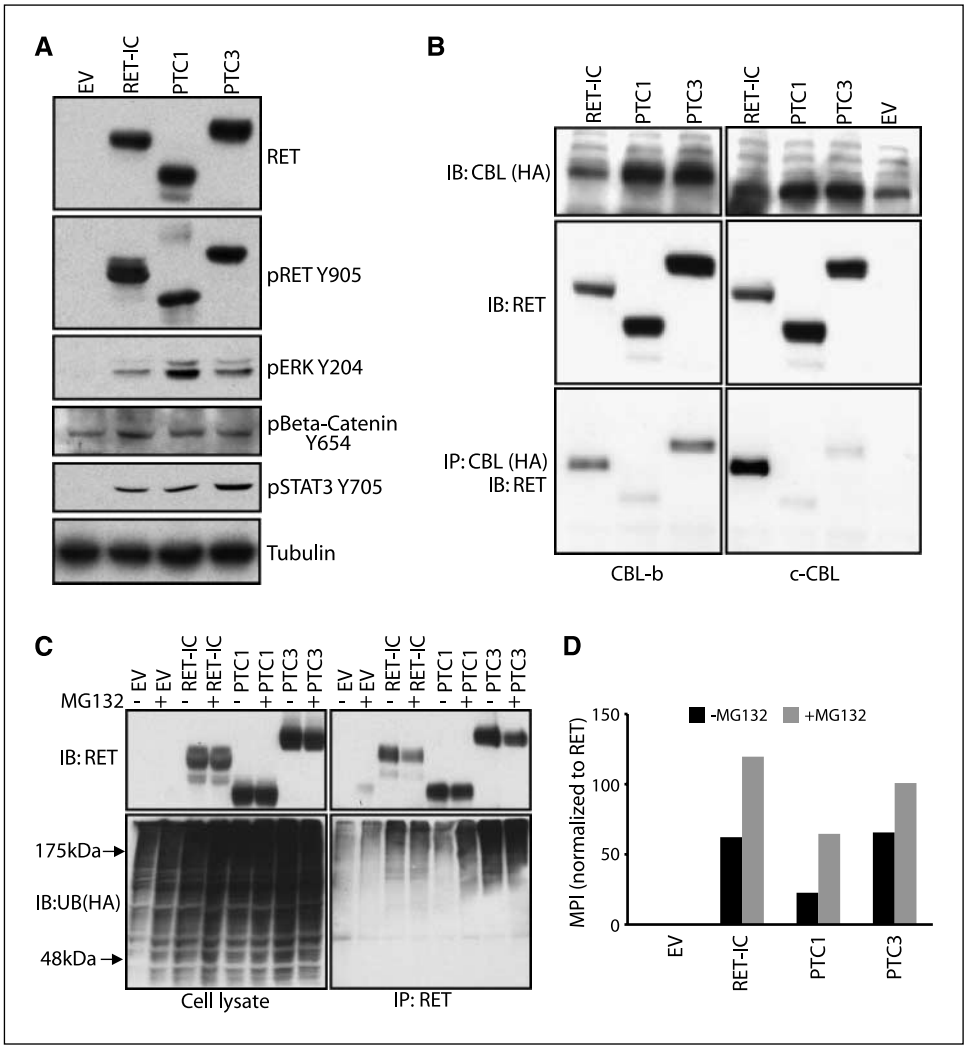

Figure 4. Characterization of RET/PTC downstream signaling and CBL interactions. *A,* lysates from transiently transfected HEK 293 Tet-on cells were separated by SDS-PAGE and immunoprobed for RET, phospho-RET (Y905), pERK1/2 (Y204), phospho-β-catenin (Y654), pSTAT3 (Y705), and γ-tubulin. *B,* cells were cotransfected with the indicated RET constructs and either c-CBL, CBL-b, or EV. Cell lysates were probed for RET and CBL (HA) expression (*top* and *middle*). CBL protein complexes were immunoprecipitated (anti-HA) and immunoblotted for RET (*bottom*). *C,* cells were cotransfected with the indicated constructs and HA-tagged ubiquitin (*UB*). MG132 was added to the indicated samples. RET-IC, PTC1, and PTC3 were immunoprecipitated (anti-RET C19). Cell lysates (*left*) and immunoprecipitates (*right*) were immunoblotted with antibodies against RET (C19) or ubiquitin (HA). *D,* mean pixel intensity of RET/ubiquitin smears in bottom right of *C* normalized to EV is plotted.

amounts of PTC3 (Fig. 4*B*). It is interesting to note that c-CBL- and CBL-b-mediated ubiquitination may have somewhat different roles. Unlike c-CBL-mediated ubiquitination, which appears to direct proteins to the lysosome for degradation, CBL-b has been shown to alter subcellular localization and inhibit interactions of cytoplasmic proteins (30–32). Further, Ettenberg and colleagues observed that overexpression of CBL-b prematurely truncates signaling through ERK/mitogen-activated protein kinase in response to epidermal growth factor, relative to cells overexpressing c-CBL (32). This would suggest that the increased affinity of CBL-b for PTC3, compared with PTC1, may limit the capacity of PTC3 for downstream signaling through ERK1/2, contributing to the lower levels of ERK/mitogen-activated protein kinase signaling relative to PTC1, which were noted above.

When normalized for total RET levels, PTC1 showed a lower degree of ubiquitination, compared with RET-IC and PTC3 (Fig. 4*C* and *D*), which is in agreement with the previous CBL-binding data (Fig. 4*B*). To ensure that ubiquitination was not an artifact of ubiquitin overexpression, ubiquitination was also measured after incubation with the proteasomal inhibitor MG132 (Fig. 4*C* and *D*). Blocking proteasome function has been shown to inhibit ubiquitin recycling and inhibit endocytosis at the late endosome sorting stage (33, 34). Together, this results in an increase in total protein ubiquitination within the cell (33, 34). MG132 was able to increase ubiquitination of all three constructs; however, PTC1 remained poorly ubiquitinated relative to RET-IC and PTC3.

Although PTC1 and PTC3 were both able to increase cell proliferation and transformation (Fig. 2*B* and *C*), they appear to mediate these effects through quantitative differences in the relative activation of similar signaling cascades. Overall, the differences in downstream signaling and ubiquitination provide explanations for the minor differences in PTC1- and PTC3-related cell proliferation and transformation observed in Fig. 2. Whether these subtle differences have an effect in an *in vivo* tumor environment is not clear. As well, the possibility that novel, presently unidentified signaling mechanism(s) induced by PTC1 and/or PTC3 mediate the observed downstream cellular effects cannot be ruled out.

PTC1 and PTC3 are expressed off relatively weak promoters. Our observations that RET/PTC expression increased signaling through growth-related pathways, cell proliferation, and transformation compared with RET-IC (Fig. 2*B* and *C*) would suggest that RET/PTCs are relatively more oncogenic than membrane-bound forms of RET. However, clinical data clearly indicate that PTCs are far less aggressive than RET-related MTCs (8). Further, Sugg and colleagues have shown that RET expression levels in primary PTC tumors correlate with oncogenicity (35). Therefore, because the promoter of the 5′ gene partner of the chimeric *RET/PTC* oncogene controls transcription of *RET/PTC*, expression of each *RET/PTC* oncogene is controlled by a different promoter. Substitution of a "foreign" promoter upstream of the RET kinase domain coding region may result in altered levels of *RET/PTC* transcript and protein expression relative to full-length RET expressed off its endogenous promoter. To investigate the expression of *RET/PTC* transcripts, we used primers 5′ or 3′ of the chromosomal breakpoints in each of *RET, CCDC6*, and *NCOA4* and spanning the *PTC1* and *PTC3* breakpoints (Supplementary Table S1; Fig. 5*A*) in qRT-PCR to amplify these regions in multiple human cancer cell lines. As expected, three cell lines, MIA-PaCa 2 (pancreatic carcinoma), SK-N-SH (neuroblastoma) and TT (MTC containing a RET MEN 2 mutation), expressed intact copies of *RET, CCDC6*, and *NCOA4* and no *PTC1* or *PTC3* rearrangement products

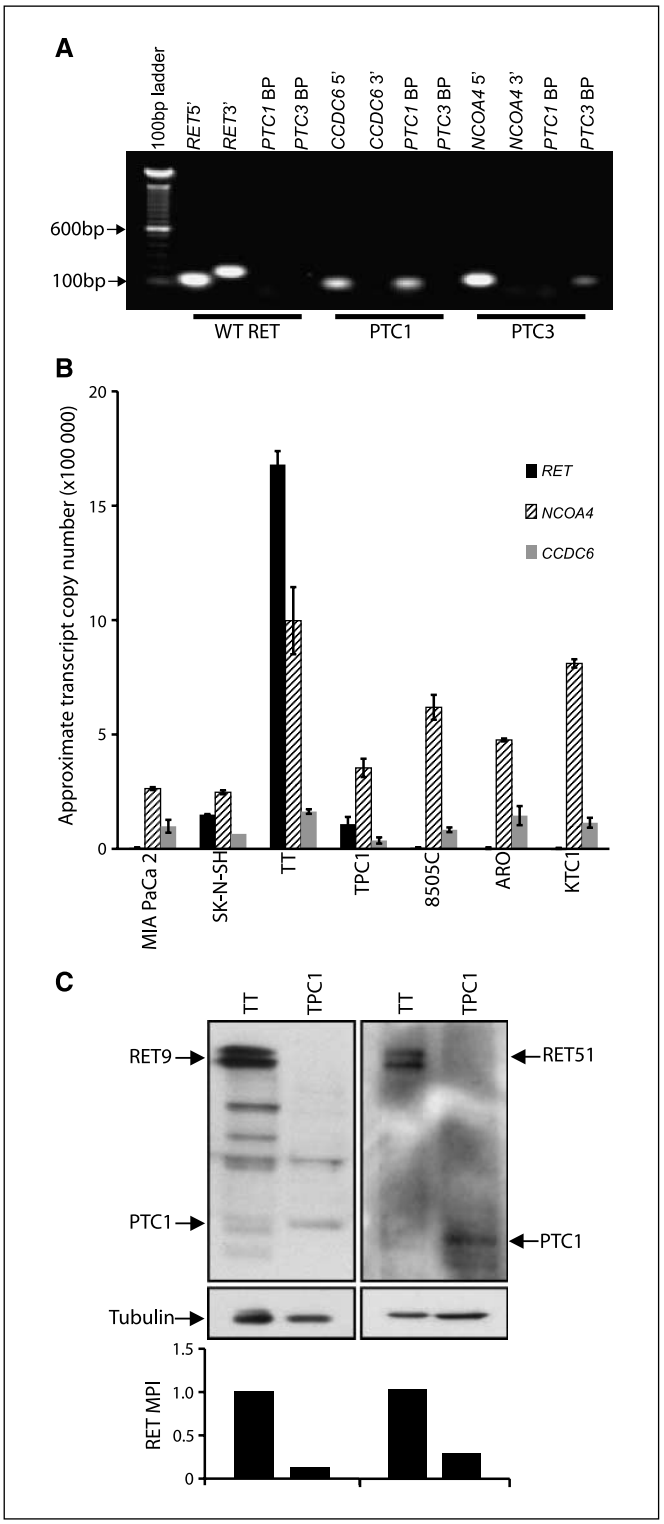

Figure 5. PTC1 and PTC3 rearrangements alter RET mRNA copy number and protein level. *A,* PCR was done on wild-type RET, PTC1, or PTC3 plasmid DNA using primer pairs listed in Supplementary Table S1. *BP,* breakpoint spanning. *B,* absolute qRT-PCR was used to estimate mRNA copy number of *RET, CCDC6*, and *NCOA4* transcripts in the indicated cell lines. Copy number was determined by fitting Ct values to a predetermined standard curve followed by normalization to *GUSB* levels in each cell line. Mean ± SD copy number was plotted ($n = 2$). *C,* cell lysates from TT and TPC1 cells were immunoblotted with two independent RET antibodies (anti-RET C19 and C20) and γ-tubulin. Densitometry comparing total RET (intensity of 175 + 155 kDa bands) with PTC1 was normalized to γ-tubulin and expressed as mean pixel intensity (*MPI*).

(Supplementary Tables S2 and S3). The TPC1 cell line (PTC containing a PTC1 rearrangement) expressed 3′ amplicons of *RET* and *NCOA4* and 5′ amplicons of *CCDC6* and *NCOA4*, was positive for a *PTC1* fusion product (Supplementary Tables S2 and S3). A second PTC cell line (KTC1) and two anaplastic thyroid carcinoma cell lines (8505C and ARO) that display characteristics of a follicular lineage expressed intact copies of *CCDC6* and *NCOA4*, barely detectable levels of full-length *RET*, and were negative for *PTC1* and *PTC3* expression (Supplementary Tables S2 and S3). Using qRT-PCR, the approximate copy number of *RET, CCDC6*, and *NCOA4* was calculated in 200 ng total RNA purified from each cell line. Copy numbers were estimated by fitting Ct values to standard curves constructed from known amounts of linearized *RET, CCDC6*, or *NCOA4* cDNA. Estimates were further normalized to *GUSB* (a housekeeping gene that is ubiquitously expressed at similar levels) Ct values as a highly sensitive control for total RNA input and RNA quality. As expected, *RET* expression varied depending on cell lineage (Fig. 5*B*). *RET* expression was highest in the TT cell line (derived from thyroid C-cells, a known site of high *RET* expression) and nearly undetectable in the thyroid follicular cell-derived lines 8505C, ARO, and KTC1 and the pancreatic derived MIA-PaCa 2 cells (Fig. 5*B*). The TPC1 cell line, which harbors a PTC1 rearrangement, expressed *RET* at a 32-fold higher level than the average of all other follicularly derived cells (8505C, ARO, and KTC1; Fig. 5*B*). However, compared with *RET* expression in TT cells, TPC1 cells still expressed 16-fold less *RET* (Fig. 5*B*). Expression of *CCDC6* was low in all cell lines, suggesting that it lies downstream of a relatively weak promoter that is poorly expressed in all cell types examined here (Fig. 5*B*). *NCOA4* expression showed variation between cell lines but was relatively higher than *CCDC6* in all cell lines. Overall, *NCOA4* expression never approached the levels of *RET* observed in the TT cell line (Fig. 5*B*), suggesting that a PTC3 rearrangement would also result in relatively lower levels of transcript as observed for the PTC1 rearrangement in the TPC1 cell line. Consistent with transcript levels, RET protein expression was reduced in the TPC1 cell line compared with TT cells as assessed with two different antibodies (Fig. 5*C*). Therefore, we predict that relatively weak promoters driving *PTC1* and *PTC3* oncogenes would lead to decreased expression of RET/PTC oncoprotein in PTC tumors relative to the endogenous RET levels found in MTCs. We believe the relatively lower transcriptional strength of *RET/PTC* oncogene promoters contributes to the indolent nature of RET/PTC tumors compared with RET-related MTCs.

Effects of altered RET activity in MTC and PTC tumors. Although beyond the scope of this study, it should be noted that MTCs and PTCs arise from different thyroid cell types (C-cells and follicular cells, respectively) and may possess intrinsic factors that promote or inhibit their relative oncogenicity. However, both cell types are epithelial in nature and metastasis of either would require an epithelial-to-mesenchymal transition and invasion through the basement membrane into surrounding tissue. Overall, when we consider the barriers to metastasis faced by both C-cells and follicular cells and the differences in downstream signaling from RET/PTCs relative to membrane-bound, activated RET (Fig. 4*A*), the correlation between relative *RET* transcript levels in MTC and PTC cell lines and the oncogenicity of their associated tumors suggests that this mechanism contributes to the indolent phenotype of RET/PTCs.

We have recently suggested that a quantitative increase in RET kinase activity may be responsible for the greater phenotypic severity of MEN 2B (RET M918T) relative to other MEN 2 mutants (13). Further, we have recently shown that MEN 2A and 2B up-regulate a similar compliment of genes; however, the more aggressive MEN 2B form induces a higher level of expression of these genes due to its increased kinase activity (36). These findings are consistent with the data presented here, although, in the case of PTCs, it appears to be a quantitative decrease in RET molecules rather than a change in intrinsic kinase activity that contributes to the lesser oncogenicity of RET/PTC tumors relative to RET-related MTCs.

Summary. To date, >25 rearrangements of RTKs that result in fusion proteins with oncogenic properties have been identified

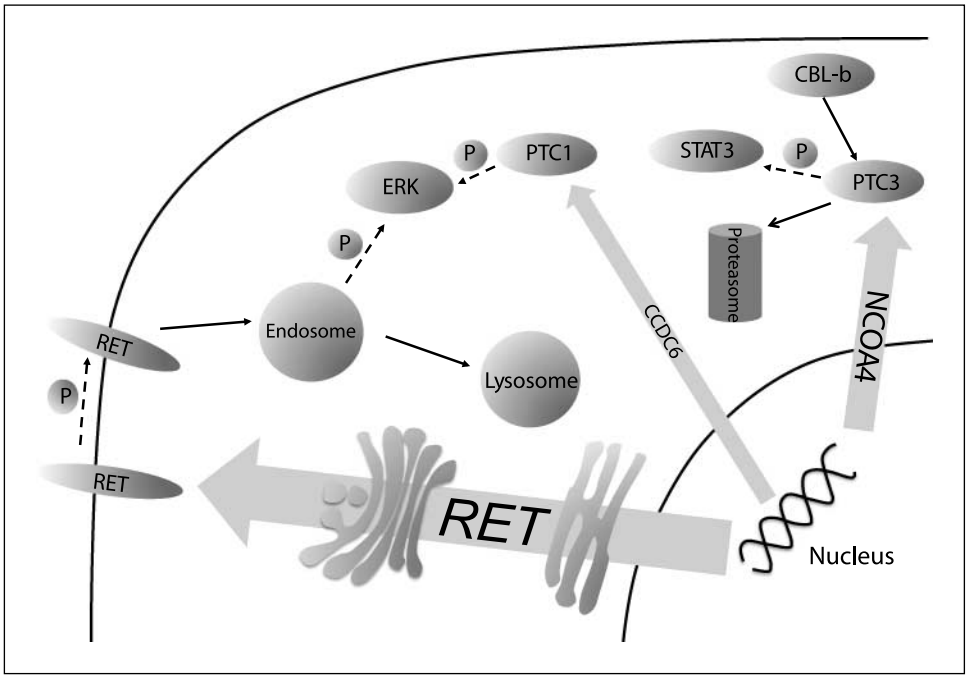

Figure 6. Characterization of RET/PTC oncogenicity. Schematic diagram highlighting important aspects of the proposed RET/PTC oncogenicity model. Full-length, endogenous, *RET* transcript is translated and targeted to the plasma membrane. On activation, it is internalized by receptor-mediated endocytosis, activates ERK from endosomes, and finally is targeted to the lysosome for degradation. PTC1 is released into the cytoplasm directly after translation. From here, it avoids degradation and promotes ERK1/2 phosphorylation. PTC3 is also delivered directly to the cytoplasm after translation, where it mediates a strong phosphorylation of STAT3, interacts with CBL-b, and may be degraded by the proteasome. *Width of gray arrows,* relative levels of transcript encoded by *RET, CCDC6*, and *NCOA4. Dashed arrows with a "P,"* regulation by phosphorylation.

(reviewed in ref. 37). Of these, *RET, PDGFR*, and *FGFR* appear to be the most promiscuous, with at least seven fusion partners identified for each (reviewed in ref. 38). Clearly, the mechanism of altered transcript levels that we describe here in relation to RET/PTCs may impact the manifestation of many rearrangement-associated cancers.

Together, our data support a model in which PTC1 and PTC3 are highly oncogenic proteins capable of up-regulating multiple canonical cell growth pathways. PTC1 and PTC3 can increase cell proliferation and produce transformation, both important steps in oncogenesis. The altered subcellular localization of RET/PTCs allows them to circumvent lysosomal degradation, promoting oncogenesis through sustained downstream signaling. However, *in vivo*, the weak promoter regions of 5′ fusion partners result in lower expression of RET/PTC mutants relative to full-length RET expressed off its endogenous promoter in RET-related MTC tumors (Fig. 6).

Disclosure of Potential Conflicts of Interest

No potential conflicts of interest were disclosed.

Acknowledgments

Received 11/19/08; revised 3/19/09; accepted 3/31/09.

Grant support: Canadian Institutes of Health Research operating grant (L.M. Mulligan), a Terry Fox Foundation studentship through the National Cancer Institute of Canada (D.S. Richardson), and a Sir Frederick Banting and Dr. Charles Best Canada Graduate Scholarship and a CIHR Traineeship in Transdisciplinary Cancer Research (T.S. Gujral).

The costs of publication of this article were defrayed in part by the payment of page charges. This article must therefore be hereby marked *advertisement* in accordance with 18 U.S.C. Section 1734 solely to indicate this fact.

We thank Drs. Sissy Jhiang, Matthew Ringel, Wallace Langdon, Stanley Lipkowitz, and Dirk Bohmann for DNA constructs; Dr. Steven Smith, Holly Spencer, and Christopher Denis for FPLC assistance; Judy Van Horne for technical assistance; Jeff Mewburn, Matthew Gordon, and Jalna Means (Queen's Cancer Research Institute Imaging Facility) for valuable input, and Drs. Bradley Webb and Waheed Sangrar provided helpful discussions.

References

1. Arighi E, Borrello MG, Sariola H. RET tyrosine kinase signaling in development and cancer. Cytokine Growth Factor Rev 2005;16:441–67.
2. Mulligan LM, Kwok JBJ, Healey CS, et al. Germ-line mutations of the RET proto-oncogene in multiple endocrine neoplasia type 2A. Nature 1993;363:458–60.
3. Hofstra RMW, Landsvater RM, Ceccherini I, et al. A mutation in the RET proto-oncogene associated with multiple endocrine neoplasia type 2B and sporadic medullary thyroid carcinoma. Nature 1994;367:375–6.
4. Takahashi M, Ritz J, Cooper GM. Activation of a novel human transforming gene, ret, by DNA rearrangement. Cell 1985;42:581–8.
5. Kondo T, Ezzat S, Asa SL. Pathogenetic mechanisms in thyroid follicular-cell neoplasia. Nat Rev Cancer 2006;6:292–306.
6. Castellone MD, Santoro M. Dysregulated RET signaling in thyroid cancer. Endocrinol Metab Clin North Am 2008;37:363–74, viii.
7. DeLellis RA, Lloyd, RV, Heitz, PU, Eng, C, editors. Pathology and genetics of tumors of endocrine origin. 1st ed. Lyon: IARC Press; 2004.
8. Soares P, Fonseca E, Wynford-Thomas D, Sobrinho-Simoes M. Sporadic ret-rearranged papillary carcinoma of the thyroid: a subset of slow growing, less aggressive thyroid neoplasms? J Pathol 1998;185:71–8.
9. Rhoden KJ, Unger K, Salvatore G, et al. RET/papillary thyroid cancer rearrangement in nonneoplastic thyrocytes: follicular cells of Hashimoto's thyroiditis share low-level recombination events with a subset of papillary carcinoma. J Clin Endocrinol Metab 2006;91:2414–23.
10. Fenton CL, Lukes Y, Nicholson D, Dinauer CA, Francis GL, Tuttle RM. The ret/PTC mutations are common in sporadic papillary thyroid carcinoma of children and young adults. J Clin Endocrinol Metab 2000;85:1170–5.
11. Bongarzone I, Vigneri P, Mariani L, Collini P, Pilotti S, Pierotti MA. RET/NTRK1 rearrangements in thyroid gland tumors of the papillary carcinoma family: correlation with clinicopathological features. Clin Cancer Res 1998;4:223–8.
12. Santoro M, Carlomagno F, Hay ID, et al. Ret oncogene activation in human thyroid neoplasms is restricted to the papillary cancer subtype. J Clin Invest 1992;89:1517–22.
13. Gujral TS, Singh VK, Jia Z, Mulligan LM. Molecular mechanisms of RET receptor-mediated oncogenesis in multiple endocrine neoplasia 2B. Cancer Res 2006;66:10741–9.
14. Gujral TS, van Veelen W, Richardson DS, et al. A novel RET kinase-β-catenin signaling pathway contributes to tumorigenesis in thyroid carcinoma. Cancer Res 2008;68:1338–46.
15. Vasko V, Espinosa AV, Scouten W, et al. Gene expression and functional evidence of epithelial-to-mesenchymal transition in papillary thyroid carcinoma invasion. Proc Natl Acad Sci U S A 2007;104:2803–8.
16. Shishido T, Akagi T, Ouchi T, Georgescu MM, Langdon WY, Hanafusa H. The kinase-deficient Src acts as a suppressor of the Abl kinase for Cbl phosphorylation. Proc Natl Acad Sci U S A 2000;97:6439–44.
17. Keane MM, Rivero-Lezcano OM, Mitchell JA, Robbins KC, Lipkowitz S. Cloning and characterization of cbl-b: a SH3 binding protein with homology to the c-cbl proto-oncogene. Oncogene 1995;10:2367–77.
18. Treier M, Staszewski LM, Bohmann D. Ubiquitin-dependent c-Jun degradation *in vivo* is mediated by the delta domain. Cell 1994;78:787–98.
19. Abramoff MD, Magelhaes PJ, Ram SJ. Image processing with ImageJ. Biophotonics Int 2004;11:36–42.
20. Chitayat S, Adams JJ, Furness HS, Bayer EA, Smith SP. The solution structure of the C-terminal modular pair from *Clostridium perfringens* μ-toxin reveals a noncellulosomal dockerin module. J Mol Biol 2008;381:1202–12.
21. Spencer DM, Graef I, Austin DJ, Schreiber SL, Crabtree GR. A general strategy for producing conditional alleles of Src-like tyrosine kinases. Proc Natl Acad Sci U S A 1995;92:9805–9.
22. Casar B, Pinto A, Crespo P. Essential role of ERK dimers in the activation of cytoplasmic but not nuclear substrates by ERK-scaffold complexes. Mol Cell 2008;31:708–21.
23. Wiley HS, Burke PM. Regulation of receptor tyrosine kinase signaling by endocytic trafficking. Traffic 2001;2:12–8.
24. Richardson DS, Lai AZ, Mulligan LM. RET ligand-induced internalization and its consequences for downstream signaling. Oncogene 2006;25:3206–11.
25. Fukuda M. Lysosomal membrane glycoproteins. Structure, biosynthesis, and intracellular trafficking. J Biol Chem 1991;266:21327–30.
26. Castellone MD, De Falco V, Rao DM, et al. The β-catenin axis integrates multiple signals downstream from RET/papillary thyroid carcinoma leading to cell proliferation. Cancer Res 2009;69:1867–76.
27. Cassinelli G, Favini E, Degl'Innocenti D, et al. RET/PTC1-driven neoplastic transformation and proinvasive phenotype of human thyrocytes involve Met induction and β-catenin nuclear translocation. Neoplasia 2009;11:10–21.
28. Schuringa JJ, Wojtachnio K, Hagens W, et al. MEN2A-RET-induced cellular transformation by activation of STAT3. Oncogene 2001;20:5350–8.
29. Scott RP, Eketjall S, Aineskog H, Ibanez CF. Distinct turnover of alternatively spliced isoforms of the RET kinase receptor mediated by differential recruitment of the Cbl ubiquitin ligase. J Biol Chem 2005;280:13442–9.
30. Fang D, Liu YC. Proteolysis-independent regulation of PI3K by Cbl-b-mediated ubiquitination in T cells. Nat Immunol 2001;2:870–5.
31. Krawczyk C, Bachmaier K, Sasaki T, et al. Cbl-b is a negative regulator of receptor clustering and raft aggregation in T cells. Immunity 2000;13:463–73.
32. Ettenberg SA, Keane MM, Nau MM, et al. cbl-b inhibits epidermal growth factor receptor signaling. Oncogene 1999;18:1855–66.
33. Melikova MS, Kondratov KA, Kornilova ES. Two different stages of epidermal growth factor (EGF) receptor endocytosis are sensitive to free ubiquitin depletion produced by proteasome inhibitor MG132. Cell Biol Int 2006;30:31–43.
34. Longva KE, Blystad FD, Stang E, Larsen AM, Johannessen LE, Madshus IH. Ubiquitination and proteasomal activity is required for transport of the EGF receptor to inner membranes of multivesicular bodies. J Cell Biol 2002;156:843–54.
35. Sugg SL, Ezzat S, Rosen IB, Freeman JL, Asa SL. Distinct multiple RET/PTC gene rearrangements in multifocal papillary thyroid neoplasia. J Clin Endocrinol Metab 1998;83:4116–22.
36. Hickey JG, Myers SM, Tian X, et al. RET-mediated gene expression pattern is affected by isoform but not oncogenic mutation. Genes Chromosomes Cancer 2009;48:429–40.
37. Lamorte L, Park M. The receptor tyrosine kinases: role in cancer progression. Surg Oncol Clin N Am 2001;10:271–88, viii.
38. Mitelman F, Johansson B, Mertens F. The impact of translocations and gene fusions on cancer causation. Nat Rev Cancer 2007;7:233–45.